Information entropic superconducting microcooler

A. O. Niskanen,[1,2,*] Y. Nakamura,[2,3,4] and J. P. Pekola[5]
[1]*VTT Technical Research Centre of Finland, Sensors, P.O. Box 1000, 02044 VTT, Finland*
[2]*CREST-JST, Kawaguchi, Saitama 332-0012, Japan*
[3]*NEC Fundamental Research Laboratories, Tsukuba, Ibaraki 305-8501, Japan*
[4]*The Institute of Physical and Chemical Research (RIKEN), Wako, Saitama 351-0198, Japan*
[5]*Low Temperature Laboratory, Helsinki University of Technology, P.O. Box 3500, 02015 TKK, Finland*
(Received 20 June 2007; revised manuscript received 15 October 2007; published 29 November 2007)

We consider a design for a cyclic microrefrigerator using a superconducting flux qubit. Adiabatic modulation of the flux combined with thermalization can be used to transfer energy from a lower temperature normal metal thin film resistor to another one at higher temperature. The frequency selectivity of photonic heat conduction is achieved by including the hot resistor as part of a high frequency *LC* resonator and the cold one as part of a low-frequency oscillator while keeping both circuits in the underdamped regime. We discuss the performance of the device in an experimentally realistic setting. This device illustrates the complementarity of information and thermodynamic entropy as the erasure of the quantum bit directly relates to the cooling of the resistor.

DOI: 10.1103/PhysRevB.76.174523 PACS number(s): 74.50.+r, 03.67.−a, 85.80.Fi

I. INTRODUCTION

For the purpose of quantum computing, the coherence properties of superconducting quantum bits (qubits) should be optimized by decoupling them from all noise sources as well as possible. However, many interesting experiments can also be envisioned when the decoupling is far from perfect. One such experiment closely related to coherence optimization is using a qubit as a spectrometer[1,3,2,4] for the environmental noise by monitoring the effect of the environment on the quantum two-level system. Here, we focus on the opposite phenomenon, i.e., the effect of a qubit on the environment. Recently, a superconducting flux qubit[5,6] with a quite small tunneling energy from the point of view of quantum computing was cooled using sideband cooling and a third level[7] from about 400 down to 3 mK. Motivated by this experiment, we consider the possibility of using a single quantum bit as a cyclic refrigerator for environmental degrees of freedom. The utilized heat conduction mechanism is photonic, which was also recently studied in the experiment.[8] Besides the possible practical uses, the device is interesting physically as it directly illustrates the connection between information entropy and thermodynamical entropy. For related superconducting coolers, see, e.g., Refs. 9–11.

II. FLUX-QUBIT COOLER AND THE THERMODYNAMIC CYCLE

We study a flux qubit coupled inductively to two different loops, as shown in Fig. 1(a). In loop j $(j=1,2)$, we have a resistor R_j in series with an inductor L_j and a capacitor C_j. These form two damped harmonic oscillators. The resistors are in general at different temperatures T_1 and T_2. The coupling of the qubit to the admittances of the two loops, Y_1 and Y_2, is assumed to be sufficiently large to dominate the relaxation of the qubit. This assumption can be easily validated by, e.g., increasing the mutual inductance. The flux qubit is an otherwise superconducting loop except for three or four Josephson junctions with suitably chosen parameters. In particular, one of the junctions is made smaller than the others to form a two-level system. When biased close to half of the flux quantum $\Phi_0=h/2e$, the qubit can be described (in persistent current basis) by the Hamiltonian

$$H/\hbar = -\frac{1}{2}(\Delta\sigma_x + \varepsilon\sigma_z), \tag{1}$$

where σ_x and σ_z are Pauli matrices, $\hbar\varepsilon=2I_p(\Phi-\Phi_0/2)$ is the flux-tunable energy bias, and Φ is the controllable flux threading the qubit loop. Away from $\Phi=\Phi_0/2$, the eigenstates have the persistent currents $\pm I_p$ circulating in the loop. The tunneling energy $\hbar\Delta$ results in an anticrossing at $\Phi=\Phi_0/2$ and there the expectation value of current of the energy eigenstates is zero. The transition angular frequency of the qubit is $\omega=\sqrt{\varepsilon^2+\Delta^2}$.

Consider the ideal cycle shown in Figs. 1(b) and 1(c) where the bias of the flux qubit is swept slowly (at a fre-

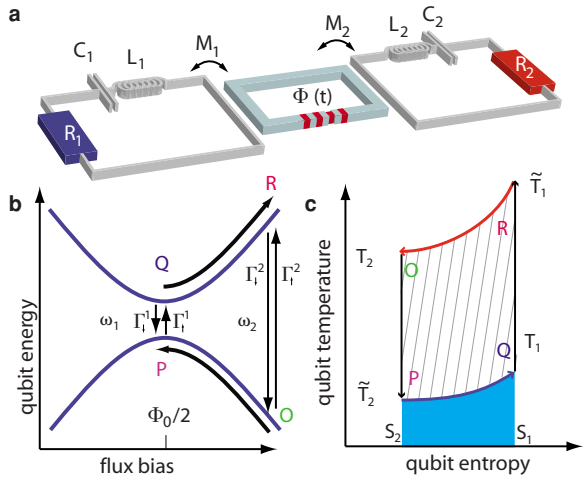

FIG. 1. (Color online) Principle of the flux-qubit cooler. (a) Layout of the circuit. (b) Energy band diagram. (c) Schematic of the cooling cycle in the qubit temperature-entropy plane.

quency f slower than $\Delta/2\pi$) between two extreme values ε_1 and ε_2 corresponding to two different energy level separations $\hbar\omega_1$ and $\hbar\omega_2$. Let us further assume that $\omega_j \approx \omega_{LCj}$ and $Q_j \gg 1$, where $\omega_{LCj}=1/\sqrt{L_jC_j}$ and $Q_j=\sqrt{L_j/C_j}/R_j$. This choice guarantees that the qubit mainly couples to resistor R_1 (R_2) at bias point 1 (2). We emphasize that although both resistors are considered baths from the point of view of qubit relaxation, only resistor 2 is strictly speaking assumed to be a heat reservoir, whereas resistor 1 has to be "small" in order to cool down. The cooling cycle consists of steps O, P, Q, and R. First, in step O, the qubit has the angular frequency ω_2 and is allowed to thermalize. Because of the bandwidth limitations imposed by the reactive elements, the qubit tends to thermalize with resistor R_2 to temperature T_2. However, ideally, the qubit splitting is large enough such that the thermal population is small. In the next step P, the flux bias is adiabatically changed to point 1 such that the level populations do not change but the energy eigenstates do. The sweep is assumed to be, however, faster than relaxation. In point 1, the angular frequency is reduced to ω_1. Because the level populations and therefore the Boltzmann factors do not change, i.e., $\hbar\omega_2/k_BT_2=\hbar\omega_1/k_B\tilde{T}_2$, the qubit must now be at a lower temperature $\tilde{T}_2$ given by $\tilde{T}_2=T_2\omega_1/\omega_2$ in order to compensate for the change of the qubit splitting. Note that the quantum mechanical adiabaticity implies also thermodynamical adiabaticity: while the energy eigenbasis changes, the level populations (and thus also the entropy) do not. In step Q, the qubit and resistor 1 are allowed to thermalize to temperature close to T_1, which results in heating of the qubit and in cooling of resistor 1 if $\tilde{T}_2<T_1$. At this point, the ideally pure quantum state of the qubit gets erased and the stored information is lost. The entropy of the qubit increases, but locally the entropy of resistor 1 decreases such that one can say that some information is "stored" in the resistor as it cools but naturally with some loss. Finally, in step R, the qubit is adiabatically shifted back to frequency ω_2, which results in heating of the qubit to the effective temperature $\tilde{T}_1=T_1\omega_2/\omega_1$, which is assumed to be higher than T_2. The excess energy is dumped to admittance 2 when the cycle starts again from the beginning. Note that due to the condition $\tilde{T}_2<T_1$, resistor 1 can never be cooled below $T_2\omega_1/\omega_2$. Since there is no isothermal stage in the above cycle, the present device is not even in principle a Carnot cooler[13] but rather an Otto-type device.[12]

The density matrix of the qubit with the transition angular frequency ω at temperature T [$\beta=(k_BT)^{-1}$] is given by

$$\rho_{\rm eq}(\beta,\varepsilon)=\frac{1}{2}\left[I+\left(\frac{\Delta}{\omega}\sigma_x+\frac{\varepsilon}{\omega}\sigma_z\right)\tanh\left(\frac{\beta\hbar\omega}{2}\right)\right], \quad (2)$$

where I is the identity matrix. Using this, the cooling power and the efficiency of the ideal cycle in Fig. 1(c) can be easily calculated. It is given by the area of the shaded region in the entropy-temperature plane below points P and Q. In principle, one could solve for the effective temperature of the qubit along the line between points P and Q as a function of entropy given by $S=-k_B\,\mathrm{Tr}(\rho\ln\rho)$. Alternatively, we can simply note that the expectation value of the energy stored in the qubit in point P is $E_P=\mathrm{Tr}[\rho_{\rm eq}(\beta_2\omega_2/\omega_1,\varepsilon_1)H_1]$, while after relaxation, we have $E_Q=\mathrm{Tr}[\rho_{\rm eq}(\beta_1,\varepsilon_1)H_1]$, where $H_1=H(\varepsilon_1)$ is the Hamiltonian at point 1. We thus get for the ideal cooling power $P=(E_Q-E_P)f$, i.e.,

$$P/f=-\frac{\hbar\omega_1}{2}\tanh\left(\frac{\beta_1\hbar\omega_1}{2}\right)+\frac{\hbar\omega_1}{2}\tanh\left(\frac{\beta_2\hbar\omega_2}{2}\right), \quad (3)$$

where f is the pump frequency. The cooling power achieves the maximum value of $\hbar\omega_1 f/2$ when the thermal population in step O (and P) is small and when the population in step Q is large, i.e., when $\beta_2\hbar\omega_2\gg 1$ and $\beta_1\hbar\omega_1\ll 1$. Naturally, a practical device has to be designed to always fulfill the first condition, in which case the smallest achievable temperature is on the order of $\hbar\omega_1/k_B$ below which the cooling power decreases rapidly. Another figure of merit is the ratio η of the heat removed from resistor 1 divided by the heat added to resistor 2. It can be obtained as the ratio of the shaded area divided by the sum of the hatched area and the shaded area, i.e., $\eta=(E_Q-E_P)/(E_R-E_O)$, where $E_O=\mathrm{Tr}[\rho_{\rm eq}(\beta_2,\varepsilon_2)H_2]$ and $E_R=\mathrm{Tr}[\rho_{\rm eq}(\beta_1\omega_1/\omega_2,\varepsilon_2)H_2]$. This simplifies neatly to $\eta=\omega_1/\omega_2<1$, which is in harmony with the second law of thermodynamics.

III. BLOCH EQUATION

For a more quantitative analysis, we have to consider the details of the relaxation rates due to the baths. The golden rule transition rates between the instantaneous ε-dependent eigenstates due to resistor j are given by

$$\Gamma^j_{\downarrow,\uparrow}=\frac{2\pi}{\hbar^2}|\langle 0;\varepsilon|dH/d\Phi|1;\varepsilon\rangle|^2M_j^2S_I^j(\pm\omega_j)$$
$$=\frac{2\pi}{\hbar^2}\frac{I_{\rm p}^2\Delta^2}{\omega^2}M_j^2S_I^j(\pm\omega_j), \quad (4)$$

where the positive sign corresponds to relaxation. The total thermalization rate is $\Gamma^j_{\rm th}=\Gamma^j_\uparrow+\Gamma^j_\downarrow$. Here, the unsymmetrized noise spectrum is given by

$$S_I^j(\omega)=\frac{1}{2\pi}\int_{-\infty}^{\infty}e^{-i\omega t}\langle\delta I_j(0)\,\delta I_j(t)\rangle dt$$
$$=\frac{1}{2\pi}\left[\frac{2\hbar\omega\,\mathrm{Re}\,Y_j(\omega)}{1-\exp(-\beta_j\hbar\omega)}\right], \quad (5)$$

where $\mathrm{Re}Y_j(\omega)=R_j^{-1}/\left[1+Q_j^2\left(\frac{\omega}{\omega_{LCj}}-\frac{\omega_{LCj}}{\omega}\right)^2\right]$ is the real part of admittance of circuit j. The total relaxation rate is thus

$$\Gamma^j_{\rm th}=\frac{2(I_{\rm p}\Delta M_j)^2\coth\left(\frac{\beta_j\hbar\omega}{2}\right)}{R_j\hbar\omega\left[1+Q_j^2\left(\frac{\omega}{\omega_{LCj}}-\frac{\omega_{LCj}}{\omega}\right)^2\right]}. \quad (6)$$

To model the behavior of the device, we utilize the Bloch master equation[14,15] given in our case by

$$\dot{\vec{M}} = -\vec{B} \times \vec{M} - \Gamma_{\text{th}}^1(\vec{M}_\parallel - \vec{M}_{T_1}) - \Gamma_{\text{th}}^2(\vec{M}_\parallel - \vec{M}_{T_2}) - \Gamma_2 \vec{M}_\perp, \tag{7}$$

where $\vec{M}=\text{Tr}(\vec{\sigma}\rho)$ is the "magnetization" of the qubit and $\vec{B}=\Delta\vec{x}+\varepsilon\vec{z}$ is the fictitious magnetic field. Note, however, that the z component of $\vec{B}$ and $\vec{M}$ do correspond to real magnetic field and magnetization, respectively. In Eq. (7), $\vec{M}_\parallel$ and $\vec{M}_\perp$ are the components of the magnetization parallel and perpendicular to $\vec{B}$, respectively. These are explicitly

$$\vec{M}_\parallel = \frac{1}{\omega^2}(\Delta M_x + \varepsilon M_z)(\Delta\vec{x} + \varepsilon\vec{z}), \tag{8}$$

$$\vec{M}_\perp = \frac{\varepsilon^2 M_x - \Delta\varepsilon M_z}{\omega^2}\vec{x} + M_y\vec{y} + \frac{\Delta^2 M_z - \Delta\varepsilon M_x}{\omega^2}\vec{z}. \tag{9}$$

Here, $\vec{M}_T$ stands for the ε-dependent equilibrium magnetization of a qubit at temperature T given explicitly by

$$\vec{M}_T = \left(\frac{\Delta}{\omega}\vec{x} + \frac{\varepsilon}{\omega}\vec{z}\right)\tanh\left(\frac{\beta\hbar\omega}{2}\right), \tag{10}$$

and $\Gamma_2=(\Gamma_{\text{th}}^1+\Gamma_{\text{th}}^2)/2$ is the dephasing rate. We neglect pure dephasing due to the intentionally large dominating thermalization rate. Equation (7) describes the dynamics of a quantum two-level system coupled to two dissipative baths. The baths tend to relax the qubit toward instantaneous equilibrium with two competing rates. Equations of this type are often used in the stationary case, but they also yield very good predictions for strong driving as, for instance, in the case of the Landau-Zener interference.[16] As is obvious from Eq. (7), the qubit actually tends to relax toward an effective ε-dependent equilibrium magnetization $(\Gamma_{\text{th}}^1\vec{M}_{T_1}+\Gamma_{\text{th}}^2\vec{M}_{T_2})/(\Gamma_{\text{th}}^1+\Gamma_{\text{th}}^2)$ at the rate $\Gamma_{\text{th}}^1+\Gamma_{\text{th}}^2$.

IV. SIMULATION RESULTS

To illustrate the practical potential of the device, we show in Fig. 2 the simulated cooling power with sinusoidal driving of $\epsilon(t)$ compared to the ideal case along with the actual loop in the entropy temperature plane. The heat flow P_j from resistor j to the qubit is simply obtained by integrating the product of the thermalization rate and the energy deficit, i.e., $P_j=f\int_0^{1/f}dt\Gamma_{\text{th}}^j(\text{Tr}\{\rho_{\text{eq}}[\beta_j,\epsilon(t)]H\}-\text{Tr}[\rho(t)H])$. The density matrix $\rho(t)=\frac{1}{2}\vec{M}(t)\cdot\vec{\sigma}$ is solved numerically using the Bloch equation (system is followed over a few periods until it has converged to the limit cycle). We see that the actual simulated behavior does not significantly deviate at low f from the ideal behavior and that cooling powers on the order of femtowatts can be achieved with reasonable sample parameters. The oscillatory behavior at high f is interpreted as the Landau-Zener interference.[16,17] The ideal operation frequency for cooling would be the highest frequency where the cycle is still fairly adiabatic, i.e., about 1 GHz is the optimal frequency in the present example.

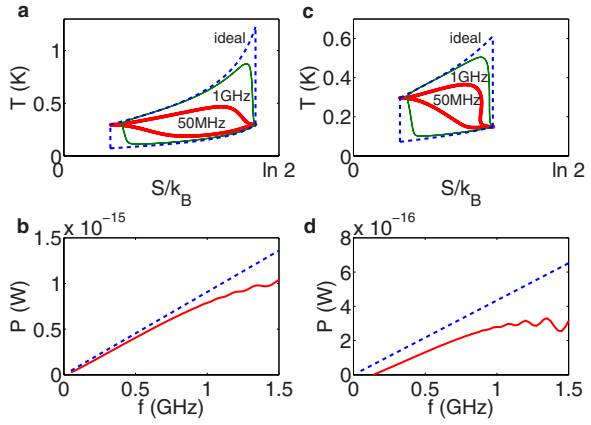

FIG. 2. (Color online) Example of the simulated cooling power. Here, $\omega_1/2\pi=\Delta/2\pi=5$ GHz ($\varepsilon=0$ GHz), $\omega_2/2\pi=20.62$ GHz ($\varepsilon=20$ GHz), $Q_1=Q_2=10$, $\omega_j=\omega_{LCj}$, and $2(I_p\Delta M_j)^2/(R_j\hbar\omega_j)=20\times10^9$ s^{-1}. This can be achieved, e.g., with $I_p=200$ nA, $M_1=29$ pH, $M_2=59$ pH, and $R_1=R_2=1$ Ω. The driving is sinusoidal. (a) The outer dashed loop illustrates the path in the T-S plane for the ideal cycle described in the text, while the thick solid line loop is a result of simulation for $f=50$ MHz. The thin solid line is a result of simulation with $f=1$ GHz. Here, $T_1=T_2=0.3\times\hbar\omega_2/k_B\approx300$ mK. (b) Simulated cooling power vs f for the same temperatures as in (a) is shown with the solid line while the dashed line is the ideal result of Eq. (3). [(c) and (d)] Same as panels (a) and (b) but with $T_1=0.5T_2\approx150$ mK. The cooling threshold at 0.14 GHz in panel (d) is caused by the finite Q factor.

However, the cooling power has to be compared with realistic heat loads to evaluate the utility of the flux-qubit cooler. On one hand, resistor 1 is subject to heat load from the phonons of the substrate on which the device rests. On the other hand, resistor 2 should be coupled well enough to phonon bath such that the unavoidable work done on it does not raise T_2 excessively. The heat flow between the electron system of resistor j and the phonon system is given by $P_{el\text{-}ph}^j=\Sigma V_j(T_j^5-T_{ph}^5)$, where V_j is the volume of resistor j and Σ is typically on the order of 10^9 W m^{-3} K^{-5}. Thus, resistor 1 needs to have a sufficiently small volume, while resistor 2 should be large enough physically in order to serve as a heat sink. In addition, the photonic heat conduction between the resistors due to temperature gradient may in principle contribute also. Following an analysis similar to Ref. 18, the heat flow from admittance $Y_2(\omega)$ to $Y_1(\omega)$ can be written as

$$P_\gamma = \int_0^\infty \frac{d\omega}{2\pi}[4\hbar\omega^3 M^2\,\text{Re}\,Y_1(\omega)\text{Re}\,Y_2(\omega)(n_2(\omega)-n_1(\omega))], \tag{11}$$

where $n_j(\omega)=[\exp(\beta_j\hbar\omega)-1]^{-1}$ are the boson occupation factors and M is the mutual inductance between the loops. For detuned well underdamped resonators, the photonic heat conduction turns out to be quite negligible. For instance, for the values of Fig. 3 with $M=5$ pH and $R_1=R_2=1$ Ω, we get only $P_\gamma=2\times10^{-18}$ W even if $T_1=0$ K and $T_2=300$ mK. Figure 2 illustrates the calculated equilibrium temperature versus operation frequency obtained numerically by finding the

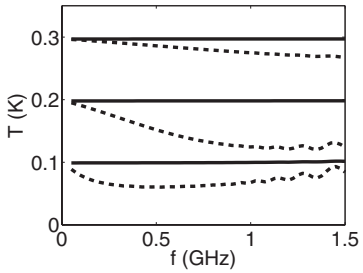

FIG. 3. Equilibrium temperature as a function of pump frequency for three different phonon bath temperatures. The temperature of resistor 1 (volume, 10^{-21} m^3) is shown with a dashed line, while the temperature of resistor 2 (volume, 10^{-18} m^3) is shown with a solid line. The bath temperatures $T_{ph} \approx T_2$ from top to bottom are $0.3 \times \hbar\omega_2/k_B$, $0.2 \times \hbar\omega_2/k_B$, and $0.1 \times \hbar\omega_2/k_B$. Otherwise, the parameters are like in Fig. 2.

balance between the dominating phononic heat conduction and the integrated cooling power. We see that almost a factor of 2 reduction of T_1 is possible with realistic parameters.

In practice, the drop of T_1 can be measured, e.g., using a SINIS (superconductor - insulator - normal metal - insulator - superconductor) thermometer,[19,20] in which resistor 1 will serve as the normal metal N. Its reading is sensitive to the electronic temperature of N only, and self-heating can be made very small. The resistors should be made out of thin film normal metal such as copper or gold with typically sub-1-Ω sq resistance. Volume can be picked freely. To get the resonant frequencies and quality factor as above, we need L_1=320 pH, C_1=3.2 pF, L_2=80 pH, and C_2=0.8 pF, which are also realistic. For the inductor, one may use either the Josephson or the kinetic inductance of superconducting wire while the capacitance values are similar to those in typical flux qubits.[2] To satisfy the conditions of the above numerical example, we need quite large mutual inductances which, however, can be easily achieved using, e.g., kinetic inductance.[21] The strong driving also requires rather large inductance between the microwave line and the qubit, which should not result in uncontrolled relaxation. For instance, M_{mw}=5 pH coupling (which is realistic) to the control line is acceptable as it would result in at most 3×10^7 s^{-1} relaxation rate assuming a 50 Ω environment at 0.3 K. This choice will not degrade the performance of the device significantly since driving is much faster. Yet, sufficiently strong driving corresponding to the example in Fig. 2 can be achieved with a modest 3 μA ac current. Fabrication process most likely will require three lithography steps.

V. CONCLUSIONS

In conclusion, we have described a method of using a superconducting flux qubit driven strongly, yet adiabatically, at microwave frequency to cool an external metal resistor. Here we considered LC resonators to achieve the required frequency selectivity but a coplanar waveguide resonator or a mechanical oscillator could be used in principle, too. We demonstrated by a numerical example that it is possible to observe the associated temperature decrease experimentally. This effect is directly related to the loss of information and thus to the increase of entropy of the quantum bit.

ACKNOWLEDGMENT

J.P.P. thanks NanoSciERA project "NanoFridge" of EU for financial support.

*antti.niskanen@vtt.fi

[1] O. Astafiev, Yu. A. Pashkin, Y. Nakamura, T. Yamamoto, and J. S. Tsai, Phys. Rev. Lett. **93**, 267007 (2004).
[2] F. Yoshihara, K. Harrabi, A. O. Niskanen, Y. Nakamura, and J. S. Tsai, Phys. Rev. Lett. **97**, 167001 (2006).
[3] P. Bertet, I. Chiorescu, G. Burkard, K. Semba, C. J. P. M. Harmans, D. P. DiVincenzo, and J. E. Mooij, Phys. Rev. Lett. **95**, 257002 (2005).
[4] K. Kakuyanagi, T. Meno, S. Saito, H. Nakano, K. Semba, H. Takayanagi, F. Deppe, and A. Shnirman, Phys. Rev. Lett. **98**, 047004 (2007).
[5] J. E. Mooij, T. P. Orlando, L. Levitov, L. Tian, C. H. van der Wal, and S. Lloyd, Science **285**, 1036 (1999).
[6] I. Chiorescu, Y. Nakamura, C. J. P. M. Harmans, and J. E. Mooij, Science **299**, 1869 (2003).
[7] S. O. Valenzuela, W. D. Oliver, D. M. Berns, K. K. Berggren, L. S. Levitov, and T. P. Orlando, Science **314**, 1589 (2006).
[8] M. Meschke, W. Guichard, and J. P. Pekola, Nature (London) **444**, 187 (2006).
[9] J. Hauss, A. Fedorov, C. Hutter, A. Shnirman, and G. Schön, arXiv:cond-mat/0701041(unpublished).
[10] J. P. Pekola, F. Giazotto, and O. P. Saira, Phys. Rev. Lett. **98**, 037201 (2007).
[11] M. Grajcar, S. H. W. van der Ploeg, A. Izmalkov, E. Il'ichev, H.-G. Meyer, A. Fedorov, A. Shnirman, and G. Schön, arXiv:0708.0665v1 (unpublished)
[12] H. T. Quan, Y. X. Liu, C. P. Sun, and F. Nori, Phys. Rev. A **76**, 012104 (2007).
[13] M. O. Scully, M. S. Zubairy, G. S. Agarwal, and H. Walther Science **299**, 862 (2003).
[14] F. Bloch, Phys. Rev. **70**, 460 (1946).
[15] Yu. Makhlin, G. Schön, and A. Shnirman, in *New Directions in Mesoscopic Physics (Towards Nanoscience)*, edited by R. Fazio, V. F. Gantmakher, and Y. Imry (Kluwer, Dordrecht, 2003), p. 197.
[16] M. Sillanpää, T. Lehtinen, A. Paila, Yu. Makhlin, and P. Hakonen, Phys. Rev. Lett. **96**, 187002 (2006).
[17] W. D. Oliver, Y. Yu, J. C. Lee, K. K. Berggren, L. S. Levitov, and T. P. Orlando, Science **310**, 1653 (2005).
[18] D. R. Schmidt, R. J. Schoelkopf, and A. N. Cleland, Phys. Rev. Lett. **93**, 045901 (2004).
[19] M. Nahum and J. M. Martinis, Appl. Phys. Lett. **63**, 3075 (1993).
[20] F. Giazotto, T. T. Heikkila, A. Luukanen, A. M. Savin, and J. P. Pekola, Rev. Mod. Phys. **78**, 217 (2006).
[21] A. O. Niskanen, K. Harrabi, F. Yoshihara, Y. Nakamura, and J. S. Tsai, Phys. Rev. B **74**, 220503(R) (2006).